Hydrogenation Catalysts

DOI: 10.1002/anie.200500773

Heterolytic Splitting of Hydrogen with Rhodium(I) Amides**

*Pascal Maire, Torsten Büttner, Frank Breher, Pascal Le Floch, and Hansjörg Grützmacher**

Dedicated to Professor Gottfried Huttner on the occasion of his 68th birthday

The classical mechanisms for the catalytic hydrogenation of C=C double bonds with rhodium(I) or iridium(I) complexes consist of six steps: 1) ligand dissociation from the catalyst precursor, 2) oxidative addition of H_2, 3) olefin coordination, 4) insertion of the coordinated C=C bond in a Rh–H bond, 5) isomerization, and 6) reductive elimination of the product.[1] In the Halpern mechanism,[2] the olefin insertion and in the Brown mechanism the reductive elimination of the alkane is rate-determining.[3] In both mechanisms, a T-shaped 14-electron $[ML_2X]$ complex is the key intermediate which adds H_2 oxidatively in an almost barrierless exothermic reaction. The heterolytic addition of hydrogen across a metal–nitrogen bond was first investigated systematically by Fryzuk and coworkers.[4] In the meantime, this reaction has been recognized as a key step in the very efficient catalytic hydrogenation of unsaturated substrates $RR^1C{=}X$,[5–7] especially of ketones (X = O), which became known as metal–ligand bifunctional catalysis through the work of Noyori and Morris. This mechanism is different and involves: 1) heterolytic addition of H_2 across the metal–amide bond as the rate-determining step, 2) binding of $RR^1C{=}X$ in the second coordination sphere of the $MH^{\delta-}$–$NH^{\delta+}$ unit, 3) "concerted" transfer of $H^{\delta-}$ from the metal atom to the C=X carbon atom and $H^{\delta+}$ from the nitrogen atom to the X center, and 4) product release. In this mechanism no change of the formal oxidation state and no major structural changes in the first coordination sphere of the metal center occur. Combined with the possibility to isolate the species that are directly involved in

[*] Dr. P. Maire, Dr. T. Büttner, Dr. F. Breher, Prof. Dr. P. Le Floch,[+] Prof. Dr. H. Grützmacher
Department of Chemistry and Applied Biosciences
ETH-Hönggerberg, 8093 Zürich (Switzerland)
Fax: (+41) 1-633-1032
E-mail: gruetzmacher@inorg.chem.ethz.ch

[+] Permanent address:
Department of Chemistry
Laboratory "Hétéroéléments et Coordination"
UMR CNRS 7653, Ecole Polytechnique
91128 Palaiseau cedex (France)

[**] This work was supported by the LANXESS AG and the Swiss National Science Foundation. We thank our colleague A. Togni for fruitful discussions and the reviewers for valuable comments.

Supporting information for this article is available on the WWW under http://www.angewandte.org or from the author.

the catalytic cycle,[7b,8] new possibilities for rational catalyst design emerge.

Recently, we isolated rhodium(I) amide olefin complexes with a rigid tetrahedrally distorted square-planar structure.[9] In accord with a calculated high activation barrier (> 29 kcal mol^{-1}), these compounds do not split H_2 heterolytically. Here we report the syntheses of rhodium amides with a novel structure. These complexes are easily prepared in a few steps, can be isolated, split H_2 heterolytically, and are directly active hydrogenation catalysts for ketones and imines without the need for any additives.

The reaction of bis(5-*H*-dibenzo[*a*,*d*]cyclohepten-5-yl)-amine (**1**, bis(tropylidenyl)amine, trop$_2$NH)[10a] with [Rh$_2$(μ_2-Cl)$_2$(cod)$_2$] (**2**) gives the dinuclear complex [Rh$_2$(μ_2-Cl)$_2$-(trop$_2$NH)$_2$] (**3**, Scheme 1).

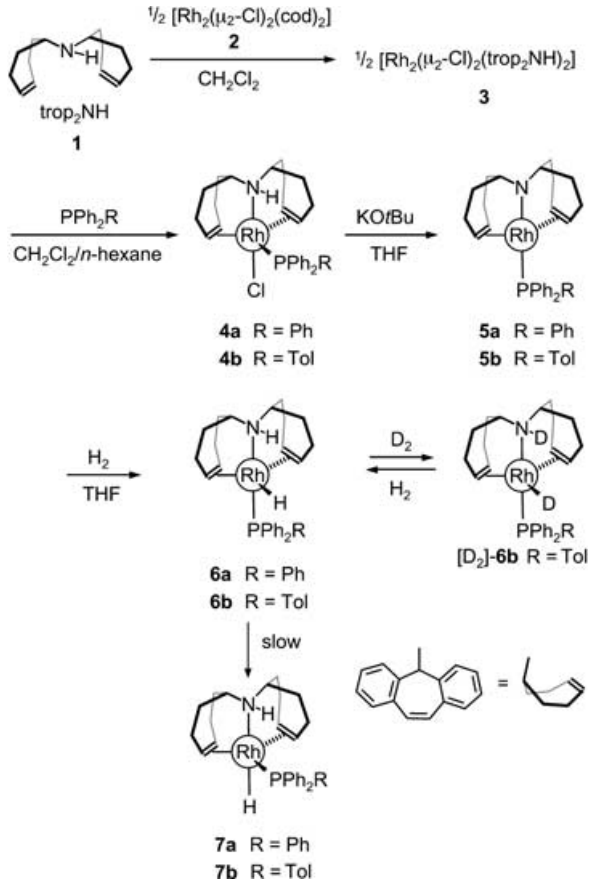

Scheme 1. Synthesis of rhodium bis(trop)amine complexes **4a**,**b**, **5a**,**b**, **6a**,**b**, and **7a**,**b**. cod = cycloocta-1,5-diene.

Subsequent reaction with a phosphane leads to the mononuclear complexes [RhCl(trop$_2$NH)(PPh$_2$R)] **4a** (R = Ph) and **4b** (R = 4-MeC$_6$H$_4$ = Tol) in which the phosphane ligand is in the equatorial position and the chloro substituent is in the apical position (these stereochemical assignments are based on the NMR spectroscopic data). The complexes **3** (red crystals) and **4a**,**b** (yellow crystals) are obtained quantitatively and can be stored in air.

The NH function of the rhodium(I)-coordinated trop$_2$NH ligands is sufficiently acidic (pK_a 15–20 in DMSO)[9,10] to be fully deprotonated by addition of one equivalent of KO*t*Bu to **4a**,**b** in THF; this is accompanied by an immediate color change of the reaction solution from orange-red to intense green. Deep green, highly air-sensitive crystals of **5a**,**b** grew from a 1:1 mixture of THF/toluene which was layered with *n*-hexane. The result of a structure analysis on a single crystal of **5b** is shown in Figure 1.[11]

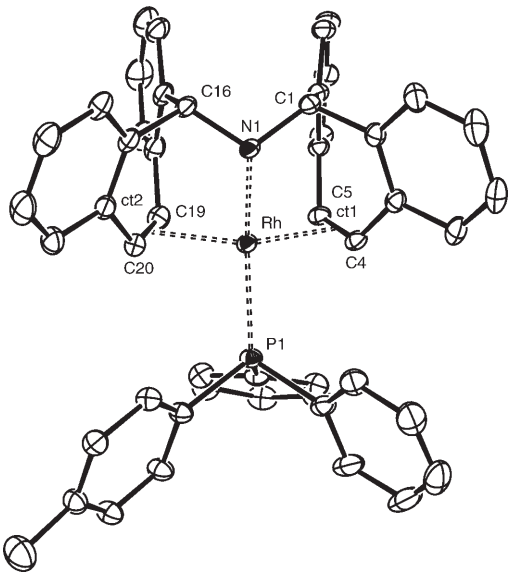

Figure 1. Structure of **5b**. Thermal ellipsoids are drawn at 30% probability; hydrogen atoms are omitted for clarity. Selected bond lengths [Å] and angles [°]: Rh–N1 2.007(1), Rh–P1 2.316(1), Rh–C5 2.165(2), Rh–C4 2.190(2), Rh–C19 2.174(2), Rh–C20 2.199(2), Rh–ct1 2.058(2), Rh–ct2 2.070(2), C4–C5 1.423(3), C19–C20 1.407(3); N1-Rh-P1 166.18(5), ct1-Rh-ct2 135.81(7), C16-N1-C1 109.5(1), C16-N1-Rh 118.5(1), C1-N1-Rh 119.0(1).

The structure of the neutral amide **5b** is unique among tetracoordinate d^8 rhodium complexes. However, a close relationship exists to the zero-valent 16 valence-electron (VE) [Ru(CO)$_2$(PR$_3$)$_2$] complexes studied by Caulton, Eisenstein, et al.[12] and to the highly reactive transient carbonyls [M(CO)$_4$] (M = Fe, Ru, Os).[13] Indeed, like these species, **5b** adopts a "sawhorse" structure with a N-Rh-P angle of 166.18(5)° and a ct1-Rh-ct2 angle of 135.81(7)° (ct = centroid of the coordinated C=C bond). Comparable angles in [Ru(CO)$_2$(P*t*Bu$_2$Me)$_2$] are: P-Ru-P 165.56(8)°, and C-Ru-C 133.3(4)°.

The amide nitrogen atom N1 has a pyramidal coordination sphere (Σ = 347°). At temperatures below 220 K, sharp and distinct ^{1}H NMR resonances for the inequivalent protons at the olefinic carbon atoms C4/C20 and C5/C19, respectively, are observed, which demonstrates that the sawhorse structure corresponds to the ground-state structure. At room temperature, these NMR resonances collapse to give one broadened singlet, indicating inversion at the nitrogen and rhodium centers, probably via a planar transition state.

The rhodium amides **5a**,**b** react rapidly and quantitatively with H_2 (1 atm) even at −78 °C to give the yellow rhodium hydride complexes [RhH(trop$_2$NH)(PPh$_2$R)] (**6a**,**b**). This reaction is very likely reversible as **6b** reacts with D_2 to give

$[D_2]$-**6b** exclusively and, vice versa, $[D_2]$-**6b** reacts with H_2 to give **6b**. The latter reaction was monitored by ^{1}H NMR spectroscopy and shows that the intensities of the signals for the NH and RhH protons build up simultaneously. We have no evidence that deuterium labeling occurs at any other position in the molecule. The structure of **6b** was determined by X-ray diffraction (Figure 2).[11]

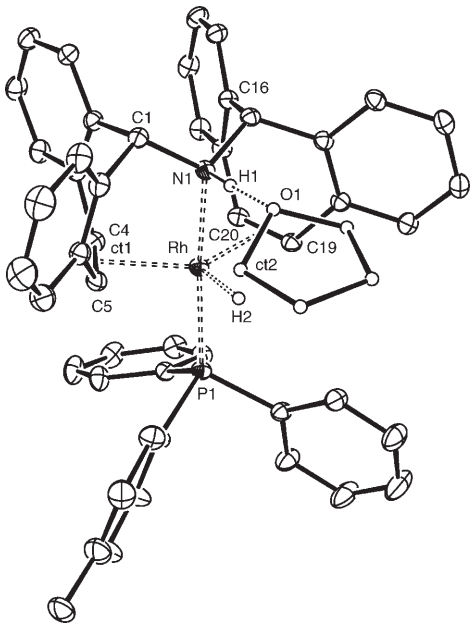

Figure 2. Structure of **6b**. Thermal ellipsoids are drawn at 30% probability; hydrogen atoms apart from H1 and H2 and one THF solvent molecule are omitted for clarity. One position of the disordered *para*-methyl substituent within the PPh_2Tol ligand is shown. Selected bond lengths [Å] and angles [°]: Rh–N1 2.178(1), Rh–P1 2.230(1), Rh–H2 1.59(3), Rh–C5 2.159(1), Rh–C4 2.199(1), Rh–C19 2.158(1), Rh–C20 2.203(1), Rh–ct1 2.057(1), Rh–ct2 2.059(1), C4–C5 1.437(2), C19–C20 1.436(2), N1···O1 3.02; N1-Rh-P1 169.95(3), ct1-Rh-ct2 132.54(5), C16-N1-C1 110.7(1), C16-N1-Rh 116.15(7), C1-N1-Rh 117.36(7).

The structural differences between **5b** and **6b** are very small. In **6b** the Rh–N bond is 9% longer and the Rh–P bond is 4% shorter than in **5b**; the ct1-Rh-ct2 angle is 2% more acute, whereas the N-Rh-P angle is 2% more open. Also the coordination sphere at N1 is not influenced very much (Σ(C-N-C, 2×C-N-Rh) = 344.2°). A THF molecule is coordinated to the NH function (N1···O1 3.02 Å) and indicates, as does the high-frequency ^{1}H NMR shift (δ: 5.56 ppm (**6a**), 5.09 ppm (**6b**)), its acidic character. The hydride ligand H2 in the equatorial position of the trigonal-bipyramidal structure of **6b** causes the typical[14] shift of the olefinic ^{13}C resonances to low frequency (by about 20 ppm) and an elongation of the coordinated C=C bonds.

Solutions of the recrystallized hydrides **6a**,**b** in THF are stable for at least 24 h. However, impurities provoke the quantitative isomerization to the air-stable yellow complexes **7a**,**b** in which the hydride ligand adopts the axial position.

The assumption that the amide complexes **5a**,**b** split H_2 heterolytically is supported by DFT calculations with the model complex $[Rh(cht_2N)(PH_3)]$ (**I**) (cht = cycloheptatrienyl, Figure 3).[15] The formation of the hydride **II** is exothermic ($\Delta_R H = -15.8$ kcal mol^{-1}) and proceeds in one step[16] via the transition state **TS-I**. The calculated NBO charges show that the H_2 molecule is significantly polarized

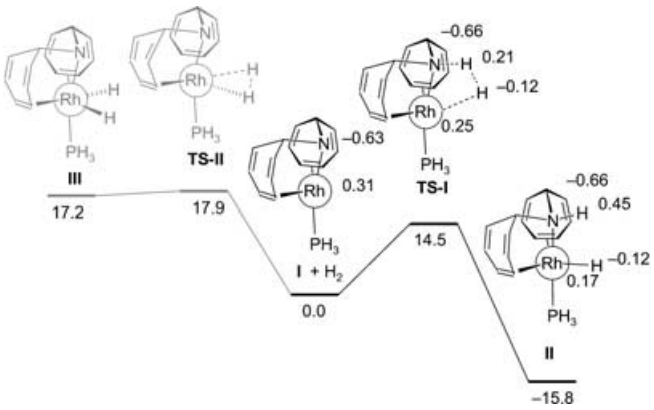

Figure 3. DFT[15] computed energies for the heterolytic (shown in black) and oxidative addition (shown in gray) of H_2 to the model complex **I**. NBO charges are given for the Rh, N, and the adding H_2 molecule in **I**, **TS-I**, and **II**.

($\Delta q^{NBO} = 0.33$ e) in the transition state (compare with $\Delta q^{NBO} = 0.57$ e in the product **II**). The polarity of the Rh^I–N bond varies little throughout this addition process ($\Delta q^{NBO} =$ 0.94 e (**I**), 0.91 e (**TS-I**), 0.83 e (**II**)). The "classical" oxidative addition of H_2 leading to the rhodium(III) dihydride **III** is an unfavorable endothermic process ($\Delta_R H = 17.9$ kcal mol^{-1}) and has to encompass the transition state **TS-II** which is higher in energy than **TS-I** by 3.4 kcal mol^{-1}.

The isolated crystalline amide **5b** and the hydride **6b** were used in catalytic hydrogenations without any further additives. The conditions and results are listed in Table 1. Under these (not yet optimized) conditions,[17] alkyl- (**8**) and aryl-substituted ketones (**9**) and the imine **10** are completely converted to the corresponding hydrogenated products cyclohexanol, 1-phenylethanol, and *N*-phenylbenzylamine, respectively. The amide **5b** and the hydride **6b** are equally active (see Table 1, entries 2 and 3). Addition of an excess of phosphine does not significantly slow down the catalytic activity. However, at the end of each catalytic run, the axial

Table 1: Hydrogenation of the ketones **8** and **9** and the imine **10** with **5b** or **6b** as catalysts.[a]

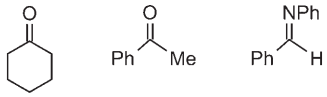

8 **9** **10**

Entry	Substrate	Cat.	S/C[b]	*t* [h]	Conversion [%]
1	**8**	**5b**	100	16	>97
2	**9**	**5b**	100	16	>97
3	**9**	**6b**	100	16	>97
4	**9**	**5b**	1000	1.5	22
5	**9**	**5b**	1000	16	65
6	**10**	**5b**	100	16	>97

[a] THF, 100 bar H_2, $T = 298$ K. [b] Ratio substrate/catalyst.

hydride **7b** is the only detectable rhodium- and phosphorus-containing species and this hydride is catalytically inactive. We therefore assume that the formation of **7b** in course of the catalytic reaction is responsible for the incomplete conversion of **9** with low catalyst loadings (Table 1, entry 5).

In summary, rhodium amides with previously unreported structures can be prepared from readily available starting materials. These complexes react cleanly with H_2 which is heterolytically split in a one-step process across the polar Rh–N bond. Both, the amide and hydride can be used directly as catalysts for ketone or imine hydrogenations, which very likely proceed via the metal–ligand bifunctional mechanism.[17] Given that the isomerization of the catalytically active hydride intermediate to an inactive one can be suppressed, efficient new catalysts for hydrogenations are in sight.

Experimental Section

The syntheses of **4a**,**b** can be performed without any particular precautions. In contrast, the amides **5a**,**b** must be handled under exclusion of moisture and oxygen. Detailed descriptions of the syntheses and spectroscopic data are given in the Supporting Information.

The reaction of **2** with two equivalents **1** in CH_2Cl_2 gave **3**·CH_2Cl_2, which was obtained as red crystals from the reaction mixture (yield > 90%). Subsequent reaction with PPh_2R (R = Ph or Tol) gave yellow solutions, from which **4a**,**b** were precipitated by addition of *n*-hexane (yields > 80%; **4a**: R = Ph, **4b**: R = Tol). The reaction of **4a**,**b** with one equivalent of KO*t*Bu in THF gave a deep green reaction solution, to which was added toluene (50 vol%). After all volatiles had been evaporated under vacuum, the green residue was extracted with THF, filtered, and concentrated. Layering this THF extract with toluene and *n*-hexane (THF/toluene/*n*-hexane = 1:1:10) gave dark green microcrystals of **5a**,**b** (yields: 80%). Deep green solutions of **5a**,**b** in THF were treated with H_2 (D_2) gas at 2 atm. Layering of the resulting yellow solutions with *n*-hexane led to the crystallization of the hydrides **6a**,**b** or [D_2]-**6b** as yellow air-stable platelets (yields > 80%).

NMR data were recorded at 298 K when not specified otherwise: **3**: M.p.: > 250 °C (decomp). ^{1}H NMR (400.1 MHz, CD_2Cl_2): $\delta = 5.97$ (dd, $^3J_{H,H} = 9.4$ Hz, $^2J_{Rh,H} = 2.1$ Hz, 4H; CH_{olefin}), 6.20 ppm (d, $^3J_{H,H} = 9.4$ Hz, 4H; CH_{olefin}); ^{13}C NMR (100.6 MHz, CD_2Cl_2): $\delta = 71.4$ ppm (br s, 8C; CH_{olefin}); ^{103}Rh NMR (12.7 MHz, CD_2Cl_2): $\delta = 2992$ ppm (s); UV/Vis (CH_3CN): λ_{max} (ε) = 232 (sh), 289 (45700), 329 nm (sh). **4a**: M.p.: > 260 °C (decomp). ^{1}H NMR (300.1 MHz, $CDCl_3$): $\delta = 1.59$ (br, 1H; NH), 5.42 (dd, $^3J_{H,H} = 9.4$ Hz, $^3J_{P,H} = 7.4$ Hz, 2H; CH_{olefin}), 5.66 ppm (ddd, $^3J_{H,H} = 9.4$ Hz, $^3J_{P,H} = 5.8$ Hz, $^2J_{Rh,H} = 1.3$ Hz, 2H; CH_{olefin}); ^{31}P NMR (101.2 MHz, $CDCl_3$): $\delta = 7.7$ ppm (d, $^1J_{Rh,P} = 111$ Hz). **4b**: M.p.: > 260 °C (decomp). In $CDCl_3$ solution two conformations (likely due to hindered rotation around the Rh–P bond) in an approximate 2:1 ratio are observed. ^{1}H NMR (300.1 MHz, $CDCl_3$): $\delta = 1.59$ (br s, 1H; NH_{maj}), 1.71 (br s, 1H; NH_{min}), 5.35–5.48 (m, 2H; $CH_{olefin,min}$; and 2H; $CH_{olefin,maj}$), 5.60–5.67 ppm (m, 2H; $CH_{olefin,min}$; and $CH_{olefin,maj}$); ^{31}P NMR (121.5 MHz, $CDCl_3$): $\delta = 6.9$ (d, $^1J_{Rh,P} = 111$ Hz, maj), 7.6 ppm (d, $^1J_{Rh,P} = 111$ Hz, min). **5a**: ^{1}H NMR (400.1 MHz, [D_8]THF, 200 K): $\delta = 4.69$ (ddd, $^3J_{H,H} = 9.0$ Hz, $^3J_{P,H} = 6.2$ Hz, $^2J_{Rh,H} = 1.2$ Hz, 2H; CH_{olefin}), 5.62 ppm (ddd, $^3J_{H,H} = 9.0$ Hz, $^2J_{Rh,H} = 3.3$ Hz, $^3J_{P,H} = 2.9$ Hz, 2H; CH_{olefin}); ^{13}C NMR (100.6 MHz, [D_8]THF, 200 K): $\delta = 76.2$ (d, $^1J_{Rh,C} = 6.7$ Hz, 2C, CH_{olefin}), 84.5 ppm (d, $^1J_{Rh,C} = 14.7$ Hz, 2C, CH_{olefin}). ^{31}P NMR (162.0 MHz, [D_8]THF, 200 K): $\delta = 40.8$ ppm (d, $^1J_{Rh,P} = 124$ Hz); ^{103}Rh NMR (12.6 MHz, [D_8]THF, 200 K): $\delta = 838$ ppm (d, $^1J_{Rh,P} = 124$ Hz); UV/Vis (THF): λ_{max} (ε) = 301 (20000), 352 (10000), 438 (3000), 662 nm (1000). **5b**: ^{1}H NMR (500.2 MHz, [D_8]THF, 190 K): $\delta = 4.74$ (dd, $^3J_{H,H} = 7.3$ Hz, $J = 7.3$ Hz, 2H; CH_{olefin}), 5.68 ppm (d, $^3J_{H,H} = 7.3$ Hz, 2H; CH_{olefin}); ^{13}C NMR (125.8 MHz, [D_8]THF, 190 K): $\delta = 75.7$ (s, 2C, CH_{olefin}), 83.9 ppm (d, $^1J_{Rh,C} = 15.1$ Hz, 2C; CH_{olefin}); ^{31}P NMR (121.5 MHz, [D_8]THF): $\delta = 38.7$ ppm (d, $^1J_{Rh,P} = 124$ Hz). **6a**: ^{1}H NMR (400.1 MHz, [D_8]THF): $\delta = -8.15$ (dd, $^1J_{Rh,H} = 23.0$ Hz, $^2J_{P,H} = 23.0$ Hz, 1H; RhH), 3.55 (d, $^3J_{H,H} = 9.3$ Hz, 2H; CH_{olefin}), 3.91 (dd, $^3J_{H,H} = 9.3$ Hz, $^3J_{H,H} = 4.7$ Hz, 2H; CH_{olefin}), 5.56 ppm (d, $^3J_{P,H} = 4.9$ Hz, 1H; NH); ^{13}C NMR (100.6 MHz, [D_8]THF): $\delta = 57.8$ (d, $^1J_{Rh,C} = 8.0$ Hz, 2C; CH_{olefin}), 60.6 ppm (d, $^1J_{Rh,C} = 8.6$ Hz, 2C; CH_{olefin}); ^{31}P NMR (162.0 MHz, [D_8]THF): $\delta = 65.4$ ppm (d, $^1J_{Rh,P} = 144$ Hz); ^{103}Rh NMR (12.6 MHz, [D_8]THF, 230 K): $\delta = -187$ ppm (d, $^1J_{Rh,P} = 144$ Hz). **6b**: M.p.: > 100 °C (decomp). ^{1}H NMR (300.1 MHz, [D_8]THF): $\delta = -8.19$ (dd, $^1J_{Rh,H} = 23.3$ Hz, $^2J_{P,H} = 23.3$ Hz, 1H; RhH), 3.65 (d, $^3J_{H,H} = 9.4$ Hz, 2H; CH_{olefin}), 3.97 (dd, $^3J_{H,H} = 9.4$ Hz, $^3J_{P,H} = 4.5$ Hz, 2H; CH_{olefin}), 5.09 ppm (d, $^3J_{P,H} = 5.5$ Hz, 1H; NH); ^{13}C NMR (75.5 MHz, [D_8]THF): $\delta = 57.0$ (d, $^1J_{Rh,C} = 7.9$ Hz, 2C; CH_{olefin}), 60.0 ppm (d, $^1J_{Rh,H} = 8.8$ Hz, 2C; CH_{olefin}); ^{31}P NMR (121.5 MHz, [D_8]THF): $\delta = 63.0$ ppm (d, $^1J_{Rh,P} = 145$ Hz); ATR IR: $\tilde{\nu} = 3169$ (m, NH), 1756 cm^{-1} (m, RhH). [D_2]-**6b**: ^{2}H NMR (46.1 MHz, THF): $\delta = -8.19$ (br s, RhD), 4.92 ppm (br s, ND); ^{31}P NMR (121.5 MHz, [D_8]THF): $\delta = 61.3$ ppm. The ND and RhD IR absorptions (expected at about 1580 and 880 cm^{-1}) are hidden by intense absorptions from the ligand. **7a**: M.p.: > 150 °C (decomp). ^{1}H NMR (400.1 MHz, [D_8]THF): $\delta = -21.37$ (dd, $^1J_{Rh,H} = 17.4$ Hz, $^2J_{P,H} = 17.4$ Hz, 1H; RhH), 0.82 (s, 1H; NH), 4.40 (dd, $^3J_{H,H} = 9.0$ Hz, $^3J_{P,H} = 7.8$ Hz, 2H; CH_{olefin}), 5.15 ppm (dd, $^3J_{H,H} = 9.0$, $^3J_{P,H} = 5.1$ Hz, 2H; CH_{olefin}); ^{13}C NMR (100.6 MHz, [D_8]THF): $\delta = 57.1$ (dd, $^2J_{P,C} = 14.7$ Hz, $^1J_{Rh,C} = 9.8$ Hz, 2C, CH_{olefin}), 61.2 ppm (dd, $^1J_{Rh,C} = 8.6$ Hz, $^2J_{P,C} = 4.90$ Hz, 2C, CH_{olefin}); ^{31}P NMR (162.0 MHz, [D_8]THF): $\delta = 47.3$ ppm (d, $^1J_{Rh,P} = 138$ Hz); ^{103}Rh NMR (12.6 MHz, [D_8]THF): $\delta = -38$ ppm (d, $^1J_{Rh,P} = 138$ Hz). **7b**: ^{1}H NMR (300.1 MHz, [D_8]THF): $\delta = -21.49$ (dd, $^1J_{Rh,H} = 17.3$ Hz, $^2J_{P,H} = 17.3$ Hz, 1H; RhH), 0.96 (s, 1H; NH), 4.47 (dd, $^3J_{H,H} = 8.8$ Hz, $^3J_{P,H} = 7.8$ Hz, 2H; CH_{olefin}), 5.20 ppm (dd, $^3J_{H,H} = 8.8$, $^3J_{P,H} = 5.0$ Hz, 2H; CH_{olefin}); ^{13}C NMR (75.5 MHz, [D_8]THF): $\delta = 56.4$ (dd, $^2J_{P,C} = 14.3$ Hz, $^1J_{Rh,C} = 9.4$ Hz, 2C; CH_{olefin}), 60.4 ppm (dd, $^1J_{Rh,C} = 8.8$ Hz, $^2J_{P,C} = 5.2$ Hz, 2C; CH_{olefin}); ^{31}P NMR (121.5 MHz, [D_8]THF): $\delta = 45.0$ ppm (d, $^1J_{Rh,P} = 138$ Hz).

Received: March 2, 2005
Revised: May 25, 2005
Published online: September 19, 2005

Keywords: amides · heterolytic H_2 splitting · homogeneous catalysis · hydrogenation · rhodium

[1] For a review citing experimental and theoretical work see: M. Torrent, M. Solà, G. Frenking, *Chem. Rev.* **2000**, *100*, 439.
[2] a) J. Halpern, *Inorg. Chim. Acta* **1981**, *50*, 11; b) For calculations see: C. Daniel, N. Koga, J. Han, X. Y. Fu, K. Morokuma, *J. Am. Chem. Soc.* **1988**, *110*, 3773.
[3] a) J. M. Brown, *Chem. Soc. Rev.* **1993**, *22*, 25; b) For calculations see: "The Challenge of d and f Electrons: Theory and Computation": N. Koga, K. Morokuma, *ACS Symp. Ser.* **1989**, *394*, 77.
[4] a) M. D. Fryzuk, P. A. MacNeil, *Organometallics* **1983**, *2*, 682; b) M. D. Fryzuk, P. A. MacNeil, S. J. Rettig, *J. Am. Chem. Soc.* **1987**, *109*, 2803; c) M. D. Fryzuk, C. D. Montgomery, *Coord. Chem. Rev.* **1989**, *95*, 1. The heterolytic splitting of H_2 by metal complexes, for example $Cu^{2+} + H_2 \rightarrow CuH^+ + H^+$ was proposed much earlier: d) J. Halpern, *J. Organomet. Chem.* **1980**, *200*, 133, and references therein; it is one key step in the enzymatic H_2 activation by metal–sulfur clusters in hydrogenases: e) D. J. Evans, C. J. Pickett, *Chem. Soc. Rev.* **2003**, *32*, 268.

[5] Recent reviews: a) S. E. Clapham, A. Hadzovic, R. H. Morris, *Coord. Chem. Rev.* **2004**, *248*, 2201; b) R. Noyori, *Angew. Chem.* **2002**, *114*, 2108; *Angew. Chem. Int. Ed.* **2002**, *41*, 2008; ; c) R. Noyori, T. Ohkuma, *Angew. Chem.* **2001**, *113*, 40; *Angew. Chem. Int. Ed.* **2001**, *40*, 40; d) M. J. Palmer, M. Wills, *Tetrahedron: Asymmetry* **1999**, *10*, 2045.

[6] Mechanistic and theoretical work: a) C. A. Sandoval, T. Ohkuma, K. Muñiz, R. Noyori, *J. Am. Chem. Soc.* **2003**, *125*, 13490, and references therein; b) K. Abdur-Rashid, S. E. Clapham, A. Hadzovic, J. N. Harvey, A. J. Lough, R. H. Morris, *J. Am. Chem. Soc.* **2002**, *124*, 15104.

[7] a) Hydrogenolysis of the iridium nitrogen bond is a key-step in the catalyzed hydrogenation of imines see: R. Dorta, D. Broggini, R. Kissner, A. Togni, *Chem. Eur. J.* **2004**, *10*, 4546, and references therein. b) See also: Y. Ng, C. Chan, J. A. Osborn, *J. Am. Chem. Soc.* **1990**, *112*, 9400.

[8] Intermediates in the related catalytic cycle for the transfer hydrogenation of ketones with ruthenium arene complexes could be isolated and crystallized, see: K.-J. Haack, S. Hashiguchi, A. Fujii, T. Ikariya, R. Noyori, *Angew. Chem.* **1997**, *109*, 297; *Angew. Chem. Int. Ed. Engl.* **1997**, *36*, 285.

[9] P. Maire, F. Breher, H. Schönberg, H. Grützmacher, *Organometallics* **2005**, *24*, 3207.

[10] a) T. Büttner, F. Breher, H. Grützmacher, *Chem. Commun.* **2004**, 2820; b) T. Büttner, J. Geier, G. Frison, J. Harmer, C. Calle, A. Schweiger, H. Schönberg, H. Grützmacher, *Science* **2005**, *307*, 235.

[11] Crystal structure of **5b**: $C_{49}H_{39}NPRh$, monoclinic, space group $P2(1)/c$; $a = 11.897(1)$, $b = 14.932(1)$, $c = 20.862(1)$ Å, $\beta = 104.046(1)°$; $V = 3595.3(2)$ Å^3; $Z = 4$; $\rho_{calcd} = 1.433$ Mg m^{-3}; crystal dimensions $0.47 \times 0.31 \times 0.25$ mm; diffractometer Bruker SMART Apex; $Mo_{K\alpha}$ radiation, 200 K, $2\Theta_{max} = 80.16°$; 97685 reflections, 22235 independent ($R_{int} = 0.0537$), direct methods; empirical absorption correction SADABS (version 2.03); refinement against full matrix (versus F^2) with SHELXTL (version 6.12) and SHELXL-97,[18] 471 parameters, $R1 = 0.0560$ and w$R2$ (all data) = 0.1471, max./min. residual electron density 1.900/−1.523 e Å^{-3}. The hydrogen atoms were placed in idealized positions and included as riding atoms. Crystal structure of **6b**: $C_{49}H_{41}NPRh \cdot 2THF$, triclinic, space group $P\bar{1}$; $a = 10.935(1)$, $b = 11.864(1)$, $c = 19.658(1)$ Å, $\alpha = 91.408(3)°$, $\beta = 100.019(3)°$, $\gamma = 109.948(3)$; $V = 2350.8(3)$ Å^3; $Z = 2$; $\rho_{calcd} = 1.301$ Mg m^{-3}; crystal dimensions $0.62 \times 0.53 \times 0.43$ mm; diffractometer Bruker SMART Apex; $Mo_{K\alpha}$ radiation, 200 K, $2\Theta_{max} = 82.46°$; 61525 reflections, 29179 independent ($R_{int} = 0.0239$), direct methods; empirical absorption correction SADABS (ver. 2.03); refinement against full matrix (versus F^2) with SHELXTL (ver. 6.12) and SHELXL-97,[18] 471 parameters, $R1 = 0.0471$ and w$R2$ (all data) = 0.1465, max./min. residual electron density 2.757/−1.422 e Å^{-3}. The hydrogen atoms were placed in idealized positions and included as riding atoms. The positions of the hydrogen atoms H1 (NH) and H2 (RhH) were obtained from a difference Fourier synthesis, they were refined isotropically. The *para*-methyl moiety of the PPh_2Tol ligand was "disordered" due to phenyl/tolyl interchange and had to be split over two positions, which were refined against each other (FVAR = 0.47). Consequently, one hydrogen atom in the *para*-position of a phenyl ring was not included in the refinement. CCDC-264482 (**5b**) and CCDC-264483 (**6b**) contain the supplementary crystallographic data for this paper. These data can be obtained free of charge from the Cambridge Crystallographic Data Centre via www.ccdc.cam.ac.uk/data_request/cif.

[12] a) M. Ogasawara, S. A. Macgregor, W. E. Streib, K. Folting, O. Eisenstein, K. G. Caulton, *J. Am. Chem. Soc.* **1996**, *118*, 10189; b) T. Gottschalk-Gaudig, J. C. Huffman, K. G. Caulton, H. Gérard, O. Eisenstein, *J. Am. Chem. Soc.* **1999**, *121*, 3242; c) T. Gottschalk-Gaudig, J. C. Huffman, H. Gérard, O. Eisenstein, K. G. Caulton, *Inorg. Chem.* **2000**, *39*, 3957.

[13] $[M(CO)_4]$: a) M = Fe, Os: M. Poliakoff, J. J. Turner, *J. Chem. Soc. Dalton Trans.* **1974**, 2276; b) M = Ru: P. L. Bogdan, E. Weitz, *J. Am. Chem. Soc.* **1989**, *111*, 3163; c) for calculations see: J. Li, G. Schreckenbach, T. Ziegler, *J. Am. Chem. Soc.* **1995**, *117*, 486. For a general discussion of the isolobal relationship between d^8ML_4 and CH_2, see: T. A. Albright, J. K. Burdett, M.-H. Whangbo, *Orbital Interactions in Chemistry*, Wiley, **1985**, pp. 360, 404.

[14] C. Böhler, N. Avarvari, H. Schönberg, M. Wörle, H. Rüegger, H. Grützmacher, *Helv. Chim. Acta* **2001**, *84*, 3127.

[15] All calculations were carried out within the framework of DFT using the Gaussian 03[15a] set of programs and the B3PW91 functional. This functional employs a combination of exchange terms: exact HF, the Becke 1988 nonlocal gradient correction[15b] and the original Slater local exchange functional.[15c] In addition, it uses the Perdew–Wang 1991 local correlation functional.[15d] The 6-31 + G* basis set was employed for all the atoms connected to the Rh center as well as for the four CH olefinic protons. All the other atoms, except Rh, were calculated using the 6-31G* basis set. A quasirelativistic effective core potential operator was used to represent the 28 innermost electrons of the rhodium atom. The basis set for the metal was that associated with the pseudopotential, with a standard double-ζ LANL2DZ contraction.[15e] Cartesian coordinates of the theoretical structures are given in the Supporting Information. The minimum energy structures were characterized by full vibration frequencies calculations. Natural charges were computed with the NBO program implemented in Gaussian 03.[15f] a) Gaussian 03 (Revision B.04), M. J. Frisch, G. W. Trucks, H. B. Schlegel, G. E. Scuseria, M. A. Robb, J. R. Cheeseman, J. A. Montgomery, Jr., T. Vreven, K. N. Kudin, J. C. Burant, J. M. Millam, S. S. Iyengar, J. Tomasi, V. Barone, B. Mennucci, M. Cossi, G. Scalmani, N. Rega, G. A. Petersson, H. Nakatsuji, M. Hada, M. Ehara, K. Toyota, R. Fukuda, J. Hasegawa, M. Ishida, T. Nakajima, Y. Honda,O. Kitao, H. Nakai, M. Klene, X. Li, J. E. Knox, H. P. Hratchian, J. B. Cross, C. Adamo, J. Jaramillo, R. Gomperts, R. E. Stratmann, O. Yazyev, A. J. Austin, R. Cammi, C. Pomelli, J. W. Ochterski, P. Y. Ayala, K. Morokuma, G. A. Voth, P. Salvador, J. J. Dannenberg, V. G. Zakrzewski, S. Dapprich, A. D. Daniels, M. C. Strain, O. Farkas, D. K. Malick, A. D. Rabuck, K. Raghavachari, J. B. Foresman, J. V. Ortiz, Q. Cui, A. G. Baboul, S. Clifford, J. Cioslowski, B. B. Stefanov, G. Liu, A. Liashenko, P. Piskorz, I. Komaromi, R. L. Martin, D. J. Fox, T. Keith, M. A. Al-Laham, C. Y. Peng, A. Nanayakkara, M. Challacombe, P. M. W. Gill, B. Johnson, W. Chen, M. W. Wong, C. Gonzalez, J. A. Pople, Gaussian, Inc., Pittsburgh, PA, **2003**; b) A. D. Becke, *Phys. Rev. A* **1988**, *38*, 3098; A. D. Becke, *J. Chem. Phys.* **1993**, *98*, 5648; c) J. C. Slater, *Quantum Theory of Molecules and Solids*, McGraw-Hill, New York, **1974**; d) J. P. Perdew, J. A. Chevary, S. H. Vosko, K. A. Jackson, M. R. Pederson, D. J. Singh, C. Fiolhais, *Phys. Rev. B* **1992**, *46*, 6671; e) P. J. Hay, W. R. Wadt, *J. Chem. Phys.* **1985**, *82*, 299; f) A. E. Reed, L. A. Curtiss, F. Weinhold, *Chem. Rev.* **1988**, *88*, 899.

[16] We could not locate any minimum structure with a η^2-bonded H_2 molecule as ligand. On the contrary, the heterolytic splitting of H_2 by ruthenium(II) phosphane amides is a two-step process including first the formation of a σ-bonded H_2 complex followed by an intramolecular proton transfer to the amide nitrogen atom (energy barrier (DFT) from the amide to the transition state for H_2 cleavage: 13.4 kcal mol^{-1}.[7b]) A one-step heterolytic cleavage of H_2 has been calculated for ruthenium(II) arene amides with a transition state at 25.2 kcal mol^{-1} (MP2): M. Yamakawa, H. Ito, R. Noyori, *J. Am. Chem. Soc.* **2000**, *122*, 1466.

[17] The complete catalytic cycle for the hydrogenation of $H_2C{=}O$ with **I** was calculated. The results strongly support the assumption that this reaction follows the metal–ligand bifunctional

mechanism and that the heterolytic H_2-splitting is the rate-determining step. The transfer of $H^{\delta+}$, $H^{\delta-}$ to the $H_2C{=}O$ molecule, which is bonded in the second coordination sphere at the place where the THF molecule is in **6b**, has only a very small barrier ($E_a = 0.5$ kcal mol^{-1}). However, our experimental set-up did not allow the stirring of the reaction mixtures, which should enhance considerably the turnover frequency. Details concerning the calculation of the catalytic cycle are given in the Supporting Information.

[18] SHELXTL, V. 6.12, Bruker AXS, Madison, Wisconsin, USA, **2002**; G. M. Sheldrick, SHELXL-97, Program for the Refinement of Crystal Structures, University of Göttingen, Germany, **1997**.

